α-Adducin Translocates to the Nucleus upon Loss of Cell-cell Adhesions

Chien-Lin Chen[1#], Yu-Ping Lin[1#], Ying-Chu Lai[1], and Hong-Chen Chen[1,2,3,4*]

[1]Department of Life Sciences, National Chung Hsing University, Taichung, Taiwan

[2]Graduate Institute of Biomedical Sciences, National Chung Hsing University, Taichung, Taiwan

[3]Department of Nutrition, China Medical University, Taichung, Taiwan

[4]Infectious Disease and Signaling Research Center, National Cheng Kung University, Tainan, Taiwan

*Corresponding author: Hong-Chen Chen, hcchen@nchu.edu.tw

#These authors contributed equally to this work.

The F-actin binding protein adducin plays an important role in plasma membrane stability, cell motility, and cell-cell junctions. In this study, we demonstrate that α-adducin is mainly localized in the nucleus of sparsely cultured epithelial cells, whereas it is localized at cell-cell junctions when the cells are grown to confluence. Disruption of cell-cell adhesions induces a nuclear translocation of α-adducin. Conversely, α-adducin is redistributed to the cytoplasm and cell-cell junctions in the process to establish cell-cell adhesions. We identify that α-adducin contains a bipartite nuclear localization signal in its COOH-terminal tail domain and a nuclear export signal in its neck region. The phosphorylation of α-adducin at Ser716 that is immediately adjacent to the nuclear localization signal appears to antagonize the function of the nuclear localization signal. Moreover, we show that depletion of α-adducin has adverse effects on cell-cell adhesions and, to our surprise, cell proliferation. The impaired cell proliferation is associated with mitotic defects characterized by disorganized mitotic spindles, aberrant chromosomal congregation/segregation, and abnormal centrosomes. Taken together, our results not only unveil the mechanism for α-adducin to shuttle between the cytoplasm and nucleus, but also highlight a potential role for α-adducin in mitosis.

Adducins comprising a protein family encoded by three closely related genes (α, β and γ) are the major components in the spectrin-based membrane cytoskeleton (1-4). The α and γ isoforms of adducins (103 kDa and 84 kDa, respectively) are ubiquitously expressed in most tissues, while the β isoform (97 kDa) has a more restricted pattern of expression, abundant in erythrocytes and the brain (1, 4, 5). The adducin isoforms are closely related in amino acid sequences and domain organization which contains an amino-terminal head domain, a neck domain, and a carboxyl-terminal tail domain (3, 4, 6). They assemble into heteromeric complexes composed of either α and β, or α and γ, through interactions in the globular amino-terminal head domains (4, 5, 7). At the end of tail domain there is a 22-residue MARCKS-related domain that has high homology to myristoylated alanine-rich C kinase substrate (MARCKS) protein (3, 4). The MARCKS-related domain is required for interactions of adducin with F-actin, spectrin, and calmodulin (3, 4, 8). The phosphorylation sites of protein kinase C (PKC) and protein kinase A (PKA) are resided in the MARCKS domain of adducin (4, 9, 10). The phosphorylation of adducin by PKC or PKA diminishes its interaction with F-actin and spectrin (10, 11).

Adducin has been implicated in development of actin assembly sites (12, 13). Adducin binds to the barbed ends (8, 14) and the sides (15) of F-actin, thereby promotes the association of spectrin with F-actin to form a spectrin-actin meshwork beneath the plasma membrane (2, 5). Dissociation of phospho-adducin releases spectrin from F-actin and leads to the exposure of F-actin barbed ends (16), rendering it possible that adducin may be involved in exposing F-actin barbed ends in motile cells. Adducin is known to play a crucial role in assembly of the membrane skeleton of erythrocytes (2, 7) and in morphological regulation during platelet activation (16, 17). In epithelial cells, α-adducin was found to localize at cell-cell contacts (9, 11) and membrane protrusions such as lamellipodia (18-20). In accordance with its subcellular localization, α-adducin has been demonstrated to be important for cell-cell junctions (21, 22) and cell motility (18, 19). In this study, we demonstrate that α-adducin contains a bipartite nuclear localization signal (NLS) and a nuclear export signal (NES) responsible for its shuttling between the nucleus and cytoplasm. Importantly, our results suggest for the first time that α-adducin may play a role in mitosis.

Results

Localization of α-adducin to cell-cell contacts or the nucleus is determined by cell density

In epithelial cells, α-adducin has been reported to distribute at lamellipodia (18-20) and cell-cell contacts (9, 11). In this study, we found that α-adducin was predominantly localized in the nucleus of sparsely cultured epithelial cells including Madin-Darby canine kidney (MDCK) cells (Figure 1A, B), human epidermal A431 cells (Figure 1C, D), and human breast epithelial MCF7 cells (Figure S1). Along with an increase in cell density, α-adducin became predominantly localized at cell-cell contacts (Figure 1A-D). We confirmed that the fluorescent signal detected by the polyclonal anti-α-adducin antibody was specific to α-adducin, because short-hairpin RNA (shRNA)-mediated knockdown of α-adducin eliminated the fluorescent signal in the nucleus (Figure 1E, F). Moreover, the relative distribution of α-adducin in the nucleus and cytoplasm was measured by cellular fractionation (Figure 1G). At low cell density, approximately 75% of total α-adducin was detected in the nuclear fraction. In contrast, at high cell density, only 10% of total α-adducin was detected in the nuclear fraction (Figure 1H). Similar to α-adducin, γ-adducin is also localized to cell-cell contacts of high density cells, but in the nucleus of low density cells (Figure S2). These results clearly indicate that subcellular distribution of α-adducin and γ-adducin at cell-cell contacts or in the nucleus can be regulated by cell density.

Co-localization of α-adducin with E-cadherin at adherens junctions relies on the integrity of the actin filaments at those sites

Confocal microscopic images taken from MDCK cells revealed that α-adducin is indeed localized at cell–cell junctions where it co-localizes with E-cadherin but not ZO-1 (Figure 2A, B), indicating that α-adducin mainly localizes at adherens junctions rather than tight junctions. As adducin is known to bind to F-actin, we wondered whether its localization at adherens junctions relies on the integrity of F-actin at these sites. Indeed, disruption of the F-actin by cytochalasin D caused a translocation of α-adducin from cell-cell junctions to the nucleus. In contrast, the localization of β-catenin at cell-cell junctions appeared to be more resistant to cytochalasin D (Figure 2C). Like α-adducin, γ-adducin relies on the integrity of F-actin in order for it to

reside at adherens junctions (Figure S2).

Sequestration of α-adducin in the nucleus by leptomycin suppresses homophilic interactions of E-cadherin and leads to less organized cell-cell junctions

To examine whether the homophilic interaction of E-cadherin is essential for recruitment of α-adducin to cell-cell junctions, a Ca^{2+} switch assay was performed in MDCK cells. The monoclonal anti-E-cadherin antibody ECCD-2, which recognizes the extracellular portion of E-cadherin, is known to preferentially recognize 'active' E-cadherin when homophilic interactions between their ectodomains are formed, whereas the monoclonal anti-E-cadherin antibody clone 36 recognizes the intracellular portion of E-cadherin (23). Depletion of Ca^{2+} from the medium, which prevented the homophilic interaction of E-cadherin, decreased the accumulation of α-adducin at cell-cell junctions, accompanied by increased accumulation of α-adducin in the nucleus (Figure 3A). Repletion of Ca^{2+} into the medium restored both homophilic interaction of E-cadherin and accumulation of α-adducin at cell-cell junctions. However, in the presence of leptomycin A, a specific inhibitor for the nucleo-cytoplasmic translocation of proteins containing a NES (24, 25), α-adducin was sequestered in the nucleus and unable to redistribute to cell-cell junctions (Figure 3A). These results together indicate that loss of E-cadherin-mediated cell–cell junctions allows translocation of α-adducin from cell-cell junctions to the nucleus. Reversely, α-adducin was exported from the nucleus to the cytoplasm and recruited to cell-cell junctions in the process to establish cell-cell adhesions. It was noted that in the presence of leptomycin, the failure of α-adducin to localize to cell-cell junctions was accompanied by the failure of E-cadherin to form homophilic interactions (Figure 3A), suggesting that the recruitment of α-adducin to cell-cell junctions may be also important for the stability of homophilic interaction between E-cadherin.

To further examine the significance of α-adducin in cell-cell junctions, MDCK cells were sparsely seeded and allowed to grow to confluence in the presence or absence of leptomycin. In the absence of leptomycin, cell-cell junctions were nicely formed, characterized by well organized α-adducin, F-actin, and β-catenin at these sites (Figure 3B). In contrast, leptomycin caused sequestration of α-adducin in the nucleus, accompanied by decreased accumulation of β-catenin and fewer organized actin filaments at cell–cell junctions, in association with increased formation of stress fibers (Figure 3B), which usually characterize weaker cell–cell adhesions. These results suggest that the recruitment of α-adducin to cell-cell contacts may be important for the formation and/or stability of cell-cell junctions. Interestingly, if MDCK cells were first allowed to grow to confluence, leptomycin was unable to sequester α-adducin in the nucleus, (Figure 3C), suggesting that once cell-cell junctions were formed, α-adducin may tightly bind to the spectrin-actin network at the lateral membrane and no longer localize to the nucleus.

α-Adducin contains a bipartite NLS in its COOH-terminal MARCKS-related domain

There are two potential NLS motifs (^{717}KKKKK^{721} and ^{729}KKSKKK^{734}) in the MARCKS-related domain of α-adducin (Figure 4A). To examine which of these two motifs is an authentic NLS for α-adducin, two lysine residues in each of the motifs were substituted with Ala. Green fluorescent protein-fused α-adducin (GFP-α-adducin) or its mutants (K718A/K719A and K730A/K732A) were transiently expressed in NIH3T3 fibroblasts in which endogenous α-adducin was not detected (data not shown). The majority (~70%) of the cells expressing GFP-α-adducin or its

K730A/K732A mutant had fluorescence in both cytoplasm and nucleus, whereas almost all the cells expressing the K718A/K719A mutant had fluorescence only in the cytoplasm (Figure 4B). These results strongly suggest that the ^{717}KKKKK^{721} motif is essential for α-adducin to localize in the nucleus. Notably, although the wild-type (wt) α-adducin was localized in both cytoplasm and nucleus, its intensity in the nucleus was stronger than in the cytoplasm. On the other hand, the intensity of the K730A/K732A mutant in the cytoplasm was stronger than in the nucleus (Figure 4B), suggesting that the ^{729}KKSKKK^{734} motif in α-adducin may also contribute to adducin's nuclear localization. Moreover, when expressed in confluent MDCK cells, GFP-α-adducin and its K718A/K719A mutant were distributed both in the cytoplasm and cell-cell contacts (Figure 4C), indicating that GFP-α-adducin is capable of targeting to cell-cell junctions of epithelial cells. To exclude the possibility that GFP fusion may somehow interfere with the subcellular localization of α-adducin, Flag-tagged α-adducin and its mutants were constructed and their localizations were examined by immunofluorescent staining with the monoclonal anti-Flag. The subcellular localization of Flag-α-adducin was similar to that of GFP-α-adducin in NIH3T3 cells (Figure 4D), indicating that GFP fusion to α-adducin does not interfere with the subcellular localization of α-adducin.

The phosphorylation of α-adducin at S716 may antagonize the function of the NLS

In addition to a bipartite NLS motif, two serine residues S716 and S726 known to be phosphorylated by PKC also reside in the MARCKS domain of α-adducin (Figure 4A). Substitution of S726 with Ala did not alter the subcellular distribution of α-adducin (Figure 4B). In contrast, substitution of S716 with Ala caused α-adducin to localize predominantly in the nucleus of NIH3T3 cells (Figure 4B, D) and MDCK cells (Figure 4C). As S716 is immediately adjacent to the ^{717}KKKKK^{721} sequence, we speculated that the phosphorylation of α-adducin at S716 may modulate the function of the NLS. To examine this possibility, S716 was substituted with Glu or Asp to mimic its phosphorylation state. The percentage of α-adducin S716A mutant, S716E mutant, and S716D mutant to localize exclusively in the nucleus was approximately 80%, 60%, and 20%, respectively (Figure 5A), indicating that α-adducin tends to localize in the cytoplasm when it carries a negative charge on S716. Moreover, the α-adducin mutant (S716D/S726D) with substitutions of both S716 and S726 with Asp was even more prone to localize in the cytoplasm than the S716D mutant (Figure 5A), suggesting that negative charges on S716 and, to a lesser extent, S726 of α-adducin may antagonize the function of the NLS.

The antibody specific to phospho-S716 or phospho-S726 of adducin (referred as anti-pS716 or anti-pS726) was used to determine whether the subcellular distribution of α-adducin is related to its phosphorylation at S716 or S726 (Figure 5B). We found that the S716 phosphorylation of α-adducin from high density cells was much higher than that from low density cells (Figure 5C). Besides, the increased S716 phosphorylation was inversely correlated with the interaction between α-adducin and importin α (Figure 5D). These data suggest that phosphorylation of α-adducin at S716 may inhibit the binding of importin α to the NLS of α-adducin, thereby preventing the nuclear translocation of α-adducin.

α-Adducin contains a NES in its neck region

Like endogenous α-adducin (Figure 3A, B), GFP-α-adducin was localized to the cytoplasm and nucleus, which can be sequestered in the nucleus by leptomycin (Figure 6C). As expected, the COOH-terminal tail domain alone, in which the

bipartite NLS is resided, was permanently localized in the nucleus regardless of leptomycin (Figure 6C). A mutant containing both neck and tail domains was preferentially localized at the cytoplasm, which can be sequestered in the nucleus by leptomycin (Figure 6C), thus suggesting that a NES may be present in the neck region. We noticed that a leucine-rich sequence (^{380}**L**MRM**L**DN**L**^{387}**)** in a motif of $LX_{(2-3)}LX_{(2-3)}$-L is present in the neck region, which resembles a NES. Indeed, deletion of this motif (aa 377-391) caused α-adducin to localize in the nucleus (Figure 6C). Together, our results indicate that α-adducin contains a NES in its neck region.

Depletion of α-adducin has adverse effects on cell-cell adhesions and cell proliferation

To examine the significance of α-adducin in epithelial cells, the expression of endogenous α-adducin was depleted by shRNA approach in A431 cells and MDCK cells (Figure 7A). Depletion of α-adducin led to a defect in cell-cell adhesions, as demonstrated by increased cell-cell dissociation (Figure 7B) and decreased cell aggregation in suspension (Figure 7C). In addition, confocal microscopic analysis revealed that depletion of α-adducin reduced the height of cells (Figure 7D). The defect in cell-cell adhesions caused by α-adducin depletion was largely rescued by re-introduction of Flag-tagged α-adducin which had been engineered to resist to the shRNA (Figure 7).

Surprisingly, depletion of α-adducin also caused a defect in cell proliferation (Figure 8A). The impaired cell proliferation was not because of increased cell death (data not shown). In addition, α-adducin depletion caused increased number of abnormal nuclei characterized by multiple, gigantic, or small appendixed nuclei (Figure 8B) and increased mitotic defects characterized by disorganized mitotic spindles, aberrant chromosomal congregation/segregation, and abnormal centrosomes (Figure 8C, D). Intriguingly, α-adducin was found to be associated with mitotic spindle (Figure 8E), suggesting a possible role for α-adducin in mitosis. The defects in cell proliferation and mitosis were largely rescued by re-expression of Flag-tagged α-adducin (Figure 8A-D). Together, our results for the first time link the function of α-adducin to cell proliferation and mitosis.

Discussion

In this study, we demonstrate that α-adducin is mainly localized in the nucleus of sparsely cultured epithelial cells, whereas it is predominantly localized at cell-cell junctions of confluent epithelial cells. Disruption of cell-cell adhesions causes a nuclear translocation of α-adducin. Conversely, α-adducin is exported from the nucleus and redistributed to cell-cell junctions in the process to establish cell-cell adhesions. We noticed that the distribution of E-cadherin, β-catenin, and F-actin at cell-cell junctions appears to be prior to the distribution of α-adducin at these sites (Figure 1 and 2). In addition, we demonstrate that the localization of α-adducin to cell-cell junctions relies on the homophilic interactions of E-cadherin (Figure 3A) and the integrity of the F-actin at cell-cell junctions (Figure 2C). Based on these results, we propose a sequential recruitment of junctional proteins to form stable adherens junctions, which is initiated by homophilic interaction between E-cadherins, followed by recruitment of β-catenin and assembly of F-actin at cell-cell junctions. Once assembled at cell-cell junctions, F-actin recruits the associations of α-adducin and spectrin, which further stabilize the structure of cell-cell junctions. Nuclear sequestration of α-adducin by leptomycin (Figure 3) or depletion of α-adducin by shRNA (Figure 7) leads to less organized cell-cell junctions and weaker cell-cell adhesions.

Together, our results support a crucial role for α-adducin in the stability of cell-cell junctions, as recently proposed by others (21, 22).

In accordance with our observation that α-adducin is localized in the nucleus upon loss of cell-cell adhesions, we demonstrate that α-adducin contains a bipartite NLS (^{717}**KKKKK**FRTPSFL**KKSKKK**^{734}) in its COOH-terminal MARCKS domain. Our results indicate that the first basic patch ^{717}KKKKK^{721} is essential for α-adducin's nuclear localization, while the second basic patch ^{729}KKSKKK^{734} appears to play a minor role in this regard (Figure 4). This bipartite NLS motif is actually conserved in all adducin isoforms. Pariser *et al.* (26) described a nuclear translocation of β-adducin stimulated by pleiotrophin, but they did not demonstrate the consensus sequence (^{704}**KKKKK**FRTPSFL**KKSKKK**^{721}) in β-adducin as a bipartite NLS. Since pleiotrophin induces disruption of cell-cell adhesions (27), the nuclear translocation of β-adducin induced by pleiotrophin (26) could be a consequence of loss of cell-cell adhesions. In consistence with this notion, we found that disruption of cell-cell adhesions of MDCK cells by hepatocyte growth factor, also known as scatter factor, is accompanied by a nuclear translocation of α-adducin (data not shown). However, the failure of leptomycin to sequester α-adducin in the nucleus of confluent cells (Figure 3C) suggests that once cell-cell junctions are established, α-adducin may tightly bind to the F-actin/spectrin networks at the lateral membrane and no longer shuttle to the nucleus.

The serine residues 716 and 726 of α-adducin are adjacent to the bipartite NLS in the MARCKS domain (Figure 4A), both of which are believed to be phosphorylation sites for PKCs. Similar to the wt α-adducin, the S726A mutant was distributed in the cytoplasm and nucleus (Figure 4B). However, the S716A mutant was predominantly localized in the nucleus (Figure 4B-D), which was hardly exported to the cytoplasm even upon formation of cell-cell adhesions (Figure 4C, 6B). In contrast to the S716A mutant, the phosphorylation mimetic mutants S716E and S716D were more prone to localize in the cytoplasm (Figure 5A). Moreover, with the anti-pS716 antibody, we demonstrate that S716 phosphorylation of α-adducin is increased upon formation of cell-cell adhesions (Figure 5C). These results together suggest that the phosphorylation of S716 may antagonize the effect of the bipartite NLS. In other words, the phosphorylation of α-adducin at S716 may favor its retention in the cytoplasm. Conversely, dephosphorylation of α-adducin on S716 may be a prerequisite for its nuclear translocation. Using the pS726-specific antibody, we demonstrate that the S726 phosphorylation in the S716A and K718A/K719A mutants remains similar even thought they are preferentially localized in the nucleus and cytoplasm, respectively (data not shown). Therefore, it is more likely that the phosphorylation of α-adducin at S716 other than S726 is involved in its regulation of subcellular localization. We have previously shown that PKCδ is the kinase responsible for S726 phosphorylation of α-adducin, which promotes formation of lamellipodia and facilitates cell migration (18). However, the identity of kinase(s) responsible for S716 phosphorylation of α-adducin remains to be identified.

Although the S716 phosphorylation of α-adducin favors its retention in the cytoplasm, as proposed in this study, its role in junctional localization of α-adducin remains obscure. Since PKC-mediated phosphorylation of adducin has been shown to decrease the affinity of adducin to the F-actin and spectrin (10, 11), it is reasonable to think that phosphorylation of α-adducin at S716 and/or S726 will diminish its association with the F-actin/spectrin network at

cell-cell junctions. However, this may not be true, because the S716D/S726D mutant retains its capability to localize at cell-cell junctions (data not shown). Therefore, it is possible that in addition to the PKC-mediated phosphorylation, other mechanisms may be involved in regulation of α-adducin's subcellular localization, in particular, at cell-cell junctions. For example, adducin is also phosphorylated by PKA (10), Rho-associated kinase (19), and Fyn, a Src family tyrosine kinase (28). The effect of α-adducin phosphorylation by different kinases on α-adducin's subcellular localization requires further studies.

In addition to NLS, we identified a NES (^{380}**L**MRM**L**DN**L**^{387}**)** in a motif of $LX_{(2-3)}LX_{(2-3)}$-L in the neck region of α-adducin (Figure 6). The α-adducin mutant with deletion of aa 377-391 is solely localized in the nucleus. Two other leucine-rich sequences (^{255}**LL**PISPEA**L**S**L**^{265} and ^{285}**L**IQKN**L**GPKSKV**LIL**RNHG**L**^{304}) are present in the head domain of α-adducin. However, deletion in these two sequences did not sequester α-adducin in the nucleus (data not shown), thus excluding the possibility of these two leucine-rich sequences as NES in α-adducin. Interestingly, while the full-length α-adducin is distributed in both cytoplasm and nucleus, the mutant without the head domain becomes predominantly localized in the cytoplasm (Figure 6C), indicating that in the absence of the head domain, the effect of NES is dominant to the effect of the NLS. These data also implicate that the head domain of α-adducin may be able to modulate the effect of the NES.

We demonstrate in this study that depletion of α-adducin has adverse effects on cell cell-cell adhesions and cell proliferation. Given α-adducin's localization at cell-cell adhesions, the result that depletion of α-adducin causes a defect in cell-cell adhesions was not surprising (Figure 7). However, the impact of α-adducin depletion to cell proliferation was not expected (Figure 8). The impaired cell proliferation caused by α-adducin depletion was found to associate with aberrances in mitosis (Figure 8). However, further studies are needed to elucidate how α-adducin exerts its function in mitosis. As α-adducin is predominantly localized in the nucleus of sparsely cultured epithelial cells, it is possible that nuclear α-adducin may facilitate cell proliferation. In fact, a number of actin-binding proteins including spectrin, the major binding partner of adducin in the cytoplasm, have been discovered to reside in the nucleus (29-31). Nuclear spectrin has been reported to play a role in chromosomal stability and DNA interstrand cross-link repair (29, 32). In addition, spectrin was reported to involve in cell cycle regulation (33). It is unclear whether α-adducin actually forms complexes with spectrin and actin in the nucleus. If this is the case, does the adducin-spectin-actin complex participate in certain nuclear processes? Nuclear actin has emerged as a new field in cell biology, which has been implicated to exert functions in transcription, chromatin dynamics, and mitosis (34-36). Our study adds α-adducin to the list of nuclear actin-binding proteins and highlights its role in cell proliferation and mitosis.

Materials and Methods

Materials

Polyclonal anti-α-adducin pS716 was generated using the synthetic peptide C-SPGKSPpSKKKKKFRT as the antigen through a custom antibody production service provided by EZBiolab, Inc. (Carmel, IN). Polyclonal anti-α-adducin (H-100), polyclonal anti-α-adducin pS726, and monoclonal anti-β-tubulin (D-10) were purchased from Santa Cruz Biotechnology. Rat monoclonal anti-E-cadherin (clone ECCD-2), mouse monoclonal anti-ZO-1 (clone ZO1-1A12)

and LipofectAMINE were purchased from Invitrogen. Mouse monoclonal anti-E-cadherin (clone 36), anti-β-catenin (clone 14), anti-PI3-kinase (the p85 subunit), and anti-importin α were purchased from BD Transduction Laboratories. Monoclonal anti-GFP was purchased from Roche. Polyclonal anti-PARP was purchased from Cell Signaling Technology. Monoclonal anti-Flag (M2), monoclonal anti-α-tubulin (DM1A), monoclonal anti-γ-tubulin (clone GTU-88), cytochalasin D, Alex-488-conjugated phalloidin, ethylene glycol-bis(β-aminoethyl ether)-N,N,N',N'-tetraacetic acid (EGTA), and puromycin were purchased from Sigma-Aldrich. Leptomycin A was purchased from Alexis Biochemicals (San Diego, CA). G418 sulfate were purchased from Calbiochem-Merck (San Diego, CA). Mounting medium with 4',6-diamidino-2-phenylindole (DAPI) was purchased from Vector Laboratories (Burlingame, CA).

Plasmid and mutagenesis

Plasmids pEGFP-C1-α-adducin and pEGFP-C1-α-adducin (S716A/S726A) were described previously (18). Plasmids pEGFP-C3-α-adducin△377-371, pEGFP-C1-α-adducin-tail (a.a. 430-737), pEGFP-C3-α-adducin–neck+tail (a.a. 350-737), and pFlag-CMV-α-adducin were constructed in our laboratory. To construct pLKO-AS2.neo-FLAG-α-adducin, the DNA fragment encoding Flag-tagged α-adducin was amplified by polymerase chain reaction using pFlag-CMV-α-adducin as the template with forward primer 5'-CTAGCTAGCACCATGGACTACAAAGACGATGACGAC-3' and reverse primer 5'-AGCTTTGTTTAAACTCAGGAGTCACTCTTCTTCTTGCTCTTC-3'and subsequently cloned into the *Nhe* I and *Pme* I site of the lentiviral vector pLKO-AS2.neo. To make Flag-α-adducin resistant to α-adducin-specific shRNA, two nucleotides were substituted with primers 5'-GATTCTGCAAAGCCCTGCGTTCTGTGAAGAATTGG-3' (T198G) and 5'-CTGCAAAGCCCTGCGTTTTGTGAAGAATTGGAATC-3' (C201T). All mutagenesis was carried out using QuikChange site-direct mutagenesis kit (Stratagene) and the desired mutations were confirmed by dideoxy DNA sequencing.

Lentivirus production and infection

The lentiviral expression system was provided by the National RNAi Core Facility, Academia Sinica, Taipei, Taiwan. To produce recombinant lentiviruses expressing α-adducin-specific shRNA, HEK293T cells were co-transfected with pLKO.1-shAdd1 (clone 84021; 2.5 μg), pCMV-ΔR8.91 (2.25 μg), and pMD.G (0.25 μg) by LipofectAMINE. To produce recombinant lentiviruses expressing Flag-α-adducin, HEK293T cells were co-transfected with pLKO-AS2.neo-Flag-adducin, pCMV-ΔR8.91, and pMD.G. To produce recombinant lentivirueses expressing luciferase-specific shRNA, HEK293T cells were co-transfected with pLKO.1-shLuc (clone 72243), pCMV-ΔR8.91, and pMD.G. After 72 h, the medium was harvested, aliquoted and stored at -80 °C.

To establish A431 cells stably expressing shRNAs specific to α-adducin, A431 cells were infected with recombinant lentiviruses encoding α-adducin-specific shRNA in the presence of 8 μg/ml polybrene (Sigma-Aldrich) for 24 h. The cells were rinsed by DMEM and allowed to grow in the growth medium for another 48 h. Subsequently, the cells were selected in the growth medium containing 2 μg/ml puromycin for one week. The puromycin-resistant cells were collected and analyzed for the expression of α-adducin proteins by immunoblotting with anti-α-adducin. To express Flag-α-adducin in the A431 cells in which endogenous α-adducin had been depleted by shRNA, the cells were infected with recombinant lentiviruses encoding

Flag-α-adducin in the presence of 8 μg/ml polybrene for 24 h. The cells were rinsed by DMEM and allowed to grow in the growth medium for another 48 h. Subsequently, the cells were selected in the growth medium containing 0.5 mg/ml G418 for one week. The neomycin-resistant cells were collected and analyzed for the expression of Flag-α-adducin by immunoblotting with anti-Flag.

Cell culture and transfection

MDCK cells, A431 cells, HEK293T cells, and NIH3T3 cells were maintained in Dulbecco's modified Eagle's medium (DMEM) supplemented with 10% fetal bovine serum and cultured at 37°C in a humidified atmosphere of 5% CO_2 and 95% air. To grow cells at low, medium, or high density, 1.0 x 10^5 of MDCK cells or A431 cells were seeded in a 6-cm culture dish for 24 h, 48 h, or 96 h, respectively.

For transient transfections, cells (5×10^5) were seeded on a 6-cm culture dish. After 18 h, the cells were incubated with the mixture of plasmid DNA (2 μg) and LipofectAMINE (10 μl) for 6 h and allowed to grow for another 36 h. To establish MDCK cells stably expressing GFP-α-adducin or its mutants, MDCK cells were transfected with the plasmid pEGFP-C1-α-adducin using LipofectAMINE. Two days after transfection, the cells were selected in the medium containing 0.5 mg/ml G418 for one week. The neomycin-resistant cells were collected and analyzed for the expression of GFP-α-adducin by immunoblotting with the monoclonal anti-GFP.

Cellular fractionation and immunoblotting

Cells were allowed to grow to confluence or sparsely seeded at 2×10^5 cells per 10-cm culture dish for one day. Cells were scraped into 1 ml hypotonic buffer (50 mM Tris, pH7.4, 10 mM NaCl, 1 mM Na_3VO_4, 1 mM phenylmethylsulfonyl fluoride, 0.2 trypsin inhibitory units/ml aprotinin, and 20 μg/ml leupeptin), homogenized by Dounce homogenizer on ice, and centrifuged at 1500 xg at 4°C for 30 min. The supernatant (as the cytoplasmic fraction) was transferred to a new tube and supplemented with SDS to a final concentration of 0.5%. The pellets were resuspended in 100 μl of hypotonic buffer with 0.5% SDS, 0.5% Triton X-100, and protease inhibitors for one hour, subjected to sonication to break chromosomal DNA, and centrifuged at 15000 xg at 4°C for 10 min. The supernatant was transferred to a new tube, which serves as the nuclear fraction. An equal proportion of lysates from the cyoplasmic and nuclear fractions was analyzed by immunoblotting with antibodies as indicated. Whole cell lysates were collected as described previously (18). Immunoblotting was performed with appropriate antibodies using the Millipore enhanced chemiluminescence system for detection. Chemiluminescent signals were detected and quantified using the Fuji LAS-3000 luminescence image system.

Calcium switch assay

For calcium switch assay, MDCK cells were grown to confluence (control) and then treated with 2.5 mM EGTA in serum-free medium for 30 min (Ca^{2+} depletion). After EGTA treatment, the medium was replaced by fresh growth medium (Ca^{2+} repletion) or by fresh growth medium supplemented with 50 nM leptomycin A (Ca^{2+} repletion+ LMA) for 4 h.

Laser-scanning confocal fluorescent microscopy

To stain α-adducin, E-cadherin, β-catenin, ZO-1, Flag-tagged proteins, and F-actin, cells were fixed in phosphate-buffered saline containing 4% paraformaldehyde for 30 minutes, permeabilized in phosphate-buffered saline containing 0.5% Triton X-100 for 10 minutes, and stained with primary

antibodies for 2 h, followed by Alex-488-conjugated, Rhodamine-conjugated, or Cy5-conjugated secondary antibodies at 4 μg/ml for 2 h. The primary antibodies used in immunofluorescence staining were diluted before use: anti-α-adducin (1:50), anti-E-cadherin (1:200), anti-ZO-1 (1:200), anti-β-catenin (1:200), anti-Flag M2 (1:200). Alex-488-conjugated phalloidin (2 μM) was used to stain F-actin. To stain mitotic spindles and centrosomes, cells were seeded at 1.0 x 10^5 cells on glass coverslips coated with type I collagen (10 μg/ml) for 48 h. Cells were permeabilized in phosphate-buffered saline containing 0.1% Triton X-100 for 2 minutes at room temperature, fixed in phosphate-buffered saline containing 4% paraformaldehyde for 30 min, and stained with anti-α-tubulin (1:500) or anti-γ-tubulin (1:500) for 2 h, followed by Alex-488-conjugated secondary antibodies at 4 μg/ml for 2 h. Coverslips were mounted in anti-fading solution with DAPI and viewed using a Zeiss LSM510 laser-scanning confocal microscope image system with a Zeiss X63 Plan-Apochromat objective.

Assays for cell proliferation, cell dissociation, and cell aggregation

For cell proliferation assay, cells (5 x 10^4) were seeded on 6-cm dishes and allowed to grow in DMEM with 10% serum. The number of the cells was enumerated every day for 5 days. For cell dissociation assay, cells were allowed to grow as discrete colonies by seeding at 2 x 10^3 per 6-cm dish. When each colony contained about 20 cells, cells were collected in serum-free medium by scarping and passed through a micropipette 15 times under constant force. The number of cell particles (*Np*) containing more than three cells was measured by using a hemocytometer. The cell suspension containing cell particles was subsequently subjected to centrifugation and trypsinization for cell number (*Nc*) measurement. The cell dissociation index was expressed as *Np/Nc* × 100%. For cell aggregation assay, cells were collected by trypsinization, suspended in DMEM supplemented with 10% serum at 10^6 cells per ml, and subjected to a constant rotation at 4 rpm in a CO_2 incubator. Three days later, the number of cell aggregates with a size larger than 150 μm in diameter was measured under a phase contrast microscope at ×40 magnification.

Statistics

Student's *t*-test was used to determine whether there was a significant difference between two means ($P < 0.05$); statistical differences are indicated with an asterisk.

Acknowledgements

This work is supported by grants NSC97-2628-B-005-001-MY3 and NSC99-2628-B-005-010-MY3 from the National Science Council, Taiwan

References

1. Gardner K, Bennett V. A new erythrocyte membrane-associated protein with calmodulin binding activity. Identification and purification. J Biol Chem 1986;261:1339-1348.
2. Gardner K, Bennett V. Modulation of spectrin–actin assembly by erythrocyte adducin. Nature 1987;328:359-362.
3. Joshi R, Gilligan DM, Otto E, McLaughlin T, Bennett V. Primary structure and domain organization of human alpha and beta adducin. J Cell Biol. 1991;115: 665-675.
4. Dong L, Chapline C, Mousseau B, Flowler L, Ramsay MK, Stevens JL, Jaken S. 35H, a sequence isolated as a protein kinase C binding protein, is a novel member of

the adducin family. J Biol Chem 1995;270:25534-25540.

5. Bennett V, Gardner K, Steiner JP. Brain adducin: a protein kinase C substrate that may mediate site-directed assembly at the spectrin-actin junction. J Biol Chem 1988;263:5860-5869.
6. Joshi R, Bennett V. Mapping the domain structure of human erythrocyte adducin. J Biol Chem 1990;265:13130-13136.
7. Hughes CA, Bennett V. Adducin: a physical model with implications for function in assembly of spectrin-actin complexes. J Biol Chem 1995;270:18990-18996.
8. Li X, Matsuoka Y, Bennett V. Adducin preferentially recruits spectrin to the fast growing ends of actin filaments in a complex requiring the MARCKS-related domain and a newly defined oligomerization domain. J Biol Chem 1998;273:19329-19338.
9. Kaiser HW, O'Keefe E, Bennett V. Adducin: Ca^{++}-dependent association with sites of cell-cell contact. J. Cell Biol. 1989;109:557-569.
10. Matsuoka Y, Hughes C A, Bennett V. Adducin regulation. Definition of the calmodulin-binding domain and sites of phosphorylation by protein kinases A and C. J Biol Chem 1996;271:25157-25166.
11. Matsuoka Y, Li X, Bennett V. Adducin is an in vivo substrate for protein kinase C: phosphorylation in the MARCKS-related domain inhibits activity in promoting spectrin-actin complexes and occurs in many cells, including dendritic spines of neurons. J Cell Biol 1998;142:485-497.
12. Falet H, Hoffmeister KM, Neujahr R, Italiano Jr JE, Stossel TP, Southwick FS, Hartwig JH. Importance of free actin filament barbed ends for Arp2/3 complex function in platelets and fibroblasts. Proc Natl Acad Sci U S A 2002;99:16782-16787.
13. Ichetovkin I, Grant W, Condeelis J. Cofilin produces newly polymerized actin filaments that are preferred for dendritic nucleation by the Arp2/3 complex. Curr Biol 2002;12:79-84.
14. Kuhlman P, Hughes C, Bennett V, Fowler V. A new function for adducin. Calcium/calmodulin-regulated capping of the barbed ends of actin filaments. J Biol Chem 1996;271:7986-7991.
15. Mische SM, Mooseker MS, Morrow JS. Erythrocyte adducin: a calmodulin-regulated actin-bundling protein that stimulates spectrin-actin binding. J Cell Biol 1987;105:2837-2845.
16. Barkalow KL, Italiano JE, Chou DE, Matsuoka Y, Bennett V, Hartwig JH. Alpha-adducin dissociates from F-actin and spectrin during platelet activation. J Cell Biol 2003;161:557-570.
17. Gilligan DM, Sarid R, Weese J. Adducin in platelets: activation-induced phosphorylation by PKC and proteolysis by calpain. Blood 2002;99:2418-2426.
18. Chen CL, Hsieh YT, Chen HC. Phosphorylation of adducin by protein kianse Cδ promotes cell motility. J Cell Sci 2007;120:1157-1167.
19. Fukata Y, Oshiro N, Kinoshita N, Kawano Y, Matsuoka Y, Bennett V, Matsuura Y, Kaibuchi K. Phosphorylation of adducin by Rho-kinase plays a crucial role in cell motility. J Cell Biol 1999;145:347-361.
20. Kiley SC, Clark KJ, Duddy SK, Welch DR, Jaken S. Increased protein kinase Cδ in mammary tumor cells: relationship to transformation and metastatic progression. Oncogene 1999;18:6748-6757.
21. Abdi KM, Bennett V. Adducin promotes micrometer-scale organization of β2-spectrin in lateral membranes of bronchial epithelial cells. Mol Biol Cell 2008;19:536-545.
22. Naydenov NG, Ivanov AI. Adducins regulate remodeling of apical junctions in human epithelial cells. Mol Biol Cell

2010;21:3506-3517.

23. Chen CL, Chen HC. Functional suppression of E-cadherin by protein kinase Cδ. J Cell Sci 2009;122:513-523.
24. Ossareh-Nazari B, Bachelerie F, Dargemont C. Evidence for a role of CRM1 in signal-mediated nuclear protein export. Science 1997;278:141-144.
25. Stade K, Ford CS, Guthrie C, Weis K. Exportin 1 (Crm1p) is an essential nuclear export factor. Cell 1997;90:1041-1050.
26. Pariser H, Herradon G, Ezquerra L, Perez-Pinera P, Deuel TF. Pleiotrophin regulates serin phosphorylation and the cellular distribution of β-adducin through activation of protein kinase C. Proc Natl Acad Sci U S A 2005;102:12407-12412.
27. Perez-Pinera P, Alcantara S, Dimitrov T, Vega JA, Deuel TF. Pleiotrophin disrupts calcium-dependent homophilic cell-cell adhesion and initiates an epithelial-mesenchymal transition. Proc Natl Acad Sci U S A 2006;103:17795-17800.
28. Shima T, Okumura N, Takao T, Satomi Y, Yagi T, Okada M, Nagai, K. Interaction of the SH2 domain of Fyn with a cytoskeletal protein, β-adducin. J Biol Chem 2001;276:42233-42240.
29. Sridharan DM, Brown M, Lambert WC, McMahon LW, Lambert MW. Nonerythroid αII spectrin is required for recruitment of FANCA and XPF to nuclear foci induced by DNA interstrand cross-links. J Cell Sci 2003;116:823-835.
30. Sridharan DM, McMahon LW, Lambert MW. αII-spectrin interacts with five groups of functionally important proteins in the nucleus. Cell Biol Intl 2006;30:866-878.
31. Young KG, Kothary R. Spectrin repeat proteins in the nucleus. BioEssays 2005;27:144-152.
32. McMahon LW, Zhang P, Sridharan DM, Lefferts JA, Lambert MW. Knockdown of αII spectrin in normal human cells by siRNA leads to chromosomal instability and decreased DNA interstrand cross-link repair. Biochem Biophys Res Commun 2009;281:288-293.
33. Metral S, Machnicka B, Bigot S, Colin Y, Dhermy D, Lecomte MC. αII-spectrin is critical for cell adhesion and cell cycle. J Biol Chem 2009;284:2409-2418.
34. Miralles F, Visa N. Actin in transcription and transcription regulation. Curr Opin Cell Biol 2006;18:261-266.
35. Chen M, Shen X. Nuclear actin and actin-related proteins in chromatin dynamics. Curr Opin Cell Biol 2007;19:326-330.
36. Zheng B, Han M, Bernier M, Wen JK. Nuclear actin and actin-binding proteins in the regulation of transcription and gene regulation. FEBS J 2009;276:2669-2685.

FIGURE LEGENDS

Figure 1: Localization of α-adducin to cell-cell contacts or the nucleus is determined by cell density. (**A**) MDCK cells (10^5) were seeded in a 6-cm culture dish, which reached low, medium, and high cell density after 24 h, 48 h, and 96 h, respectively. The cells were fixed, stained for α-adducin, β-catenin, and nucleus, and visualized by confocal microscopy. Arrowheads indicate that the recruitment of β-catenin to cell-cell contacts is prior to the recruitment of

α-adducin to those sites. Scale bars: 20 μm. (**B**) MDCK cells were grown as described in panel A and stained for α-adducin, F-actin, and nucleus. Arrowheads indicate that the formation of the F-actin at cell-cell junctions is a precedent event to the recruitment of α-adducin to those sites. (**C**) A431 cells (10^5) were seeded in a 6-cm culture dish, which reached low, medium, and high cell density after 24 h, 48 h, and 96 h, respectively. The cells were stained for α-adducin, β-catenin, and nucleus. Scale bars: 20 μm. (**D**) A431 were grown as described in panel C and stained for α-adducin, F-actin, and nucleus. (**E**) A431 cells were infected by recombinant lentiviruses expressing shRNAs specific to α-adducin (*shAdd*) or luciferase (*shLuc*) as a control. An equal amount of whole cell lysates was analyzed by immunoblotting with anti-α-adducin or anti-β-tubulin. (**F**) A431 cells and those harboring shRNAs specific to α-adducin (shAdd) or luciferase (shLuc) were sparely cultured and stained for α-adducin and nucleus. Note that α-adducin knockdown substantially eliminates the fluorescent signal of α-adducin. (**G**) A431 cells were grown at low or high density. Whole cell lystaes (*Total*) were fractionated into cytoplasmic (*Cyto*) and nuclear (*N*) fractions, as described in Materials and Methods. An equal proportion of cell lysates from different fractions was analyzed by immunoblotting with antibodies to α-adducin, polyadenosine diphosphate-ribose polymerase (PARP; as a nuclear marker), or the p85 subunit of phosphatidylinositol 3-kinase (p85; as a cytoplasmic marker). (**H**) Quantitative presentation for relative distribution of α-adducin in the cytoplasmic fraction (*Cyto*) and the nuclear fraction (*N*) from A431 cells grown at low or high density. Values (means ± s.d.) are from three independent experiments. *P< 0.05.

Figure 2: Co-localization of α-adducin with E-cadherin at adherens junctions relies on the integrity of the actin filaments at those sites. (**A**) MDCK cells were grown to confluence and stained for α-adducin, E-cadherin, β-catenin, and nucleus. Arrowheads indicate that the presence of α-adducin at cell-cell junctions is preceded by E-cadherin and β-catenin. Scale bars: 20 μm. (**B**) MDCK cells were grown to confluence and stained for α-adducin, E-cadherin, and ZO-1. White line on the confocal XY-section image represents the region where confocal XZ-section images were taken. The XZ-section images reveal that α-adducin co-localizes with E-cadherin, but not ZO-1, at cell–cell junctions. Scale bars: 20 μm. (**C**) MDCK cells were grown to confluence, treated with 10 μM cytochalasin D (*Cyto. D*) for various times as indicated, and then stained for α-adducin, β-catenin, F-actin, and nucleus. Note that disruption of the F-actin at cell-cell junctions causes a translocation of α-adducin to the nucleus. Scale bars: 20 μm.

Figure 3: α-adducin shuttles between cell-cell junctions and the nucleus. (**A**) MDCK cells were grown to confluence (*control*) and then treated with 2.5 mM EGTA in serum-free medium for 30 min (Ca^{2+} *depletion*). After EGTA treatment, the medium was replaced by fresh growth medium (Ca^{2+} *repletion*) or by fresh growth medium supplemented with 50 nM leptomycin A (Ca^{2+} *repletion+ LMA)* for 4 h. The cells were fixed and stained for α-adducin, E-cadherin, and nucleus. A rat monoclonal antibody (clone ECCD-2) and a mouse monoclonal antibody (clone 36) were used to stain E-cadherin. Note that the ECCD-2 antibody recognizes the extracellular domain of E-cadherin and the clone 36 antibody recognizes the intracellular domain of E-cadherin. Scale bars: 20 μm. (**B**) MDCK cells were grown at low cell density (10^5 per 6-cm culture dish) for 48 h and then treated with (+) or without (-) 50 nM leptomycin A

(*LMA*) for another 10 h. The cells were fixed and stained for α-adducin, β-catenin, F-actin, and nucleus. Scale bars: 20 μm. (**C**) MDCK cells were seeded at high cell density (7 x 10^5 per 6-cm culture dish) for 48 h and then treated with (+) or without (-) 50 nM leptomycin A (*LMA*) for another 10 h. The cells were fixed and stained for α-adducin, β-catenin, F-actin, and nucleus. Scale bars: 20 μm.

Figure 4: α-Adducin contains a bipartite NLS in its COOH-terminal MARCKS-related domain. (**A**) Diagram depicts the domain structure of α-adducin. The COOH-terminal tail domain of α-adducin contains a highly basic stretch (+++) of 27 amino acids (aa 711-737) with sequence similar to a domain in the myristoylated alanine-rich C kinase substrate (MARCKS). A bipartite NLS motif is marked, which is conserved in α, β, and γ adducins. (**B**) GFP-α-adducin and its mutants were transiently expressed in NIH3T3 cells and their distributions in the nucleus alone (*N*), the cytoplasm alone (*C*), or both nucleus and cytoplasm (*N*+*C*) were measured. Values (means ± s.d.) are from three independent experiments (n>300). Scale bars: 20 μm. (**C**) MDCK cells stably expressing GFP-α-adducin or its mutants were grown to confluence and the green fluorescence was visualized under a confocal microscope. Scale bars: 20 μm. (**D**) Flag-tagged α-adducin and its mutants were transiently expressed in NIH3T3 cells and detected by immunofluorescent staining with anti-Flag. The distribution of Flag-tagged α-adducin in the nucleus alone (*N*), the cytoplasm alone (*C*), or both nucleus and cytoplasm (*N*+*C*) were measured. Values (means ± s.d.) are from three independent experiments (n>200). Scale bars: 20 μm.

Figure 5: The phosphorylation of α-adducin at S716 may antagonize the function of its NLS. (**A**) GFP-α-adducin S716 mutants were transiently expressed in NIH3T3 cells and their distributions in the nucleus alone (*N*), the cytoplasm alone (*C*), or both nucleus and cytoplasm (*N*+*C*) were measured. Values (means ± s.d.) are from three independent experiments (n>200). Scale bars: 20 μm. (**B**) GFP-α-adducin and its mutants were transiently expressed in HEK293 cells. An equal amount of whole cell lysates was analyzed by immunoblotting with antibodies specific to phosphorylated Ser716 or Ser726 (pS716 or pS726) in α-adducin. (**C**) An equal amount of whole cell lysates from A431 cells at low or high cell density was analyzed by immunoblotting with antibodies as indicated. The phosphorylation of endogenous α-adducin at S716 or S726 was detected by phospho-specific antibodies and expressed as –fold relative to the level of the cells at low cell density. (**D**) The interaction between α-adducin and importin α was analyzed by co-immunoprecipitation. IP, immunoprecipitation; IB, immunoblotting. The result shown is the representative from three experiments.

Figure 6: Identification of a NES in the neck region of α-adducin. (**A**) Diagram depicts the domain structure of GFP-fused α-adducin and its mutants. The mutant containing the neck and tail domains was designated as “neck + tail”. The mutant with deletion of aa 377-391 was designated as △377-391. WT, wild-type. (**B**) GFP-α-adducin and its mutants were transiently expressed in 293 cells for two days. The cells were lyzed and an equal amount of whole cell lysates was analyzed by immunoblotting with antibodies as indicated. (**C**) GFP-α-adducin or its mutants were

transiently expressed in subconfluent MDCK cells for 12 h and then the cells were treated with (+) or without (-) 50 nM leptomycin A (*LMA*) for 5 h. The cells were fixed and the fluorescence of GFP-α-adducin was visualized under a fluorescent microscope. The images shown are representative from two experiments. Scale bars: 10 μm

Figure 7: Depletion of α-adducin has an adverse effect on cell-cell adhesions. (**A**) A431 cells and MDCK cells were infected with recombinant lentiviruses expressing shRNAs specific to α-adducin (*shAdd*) or luciferase (*shLuc*) as a control. Flag-tagged α-adducin was re-introduced into the cells in which endogenous α-adducin had been depleted. The cells with Flag-α-adducin were designated as shAdd/Flag-Add. An equal amount of whole cell lysates was analyzed by immunoblotting with antibodies as indicated. (**B**) Cell dissociation assay. The cells were allowed to grow as discrete colonies. Cell colonies were collected in serum-free medium by scraping and then passed through a micropipette 15 times under constant force. The number of cell particles (*Np*) containing more than three cells was measured under a hemocytometer. The cell suspension containing cell particles was subsequently subjected to centrifugation and trypsinization for cell number (*Nc*) measurement. The cell dissociation index was expressed as *Np/Nc* × 100%. Values (means ± s.d.) are from three independent experiments. **P*< 0.05. Scale bars: 100 μm (**C**) Cell aggregation assay. The cells were collected by trypsinization, suspended in medium with 10% serum, and subjected to a constant rotation. Three days later, the number of cell aggregates with a size larger than 150 μm in diameter was measured under a phase contrast microscope. Values (means ± s.d.) are from three independent experiments. **P* < 0.05. (**D**) An equal numbers of the cells were seeded on glass coverslips. 24 h later, the cells were fixed and stained for E-cadherin. The XZ-section images of the cells were obtained by confocal microscopy and the height of the cells were measured. Values (means ± s.d.) are from three independent experiments (n>100). **P* < 0.05.

Figure 8: Depletion of α-adducin impairs cell proliferation, associated with mitotic defects. (**A**) A431 cells, MDCK cells, and A549 cells were infected with recombinant lentiviruses expressing shRNAs specific to α-adducin (*shAdd*) or luciferase (*shLuc*) as a control. Flag-tagged α-adducin was re-introduced into the cells in which endogenous α-adducin had been depleted (*shAdd/Flag-Add*). An equal number of cells were grown in the medium with 10% serum and the number of cells was counted after 4 days. Data are expressed as percentage relative to the control cells, which is defined as 100%. Values (means ± s.d.) are from three independent experiments. **P* < 0.05. (**B**) A431 cells and those expressing shAdd, shLuc, or Flag-Add were fixed and stained for DNA. The percentage of cells with abnormal nucleus in total counted cells (n > 200) was measured. Note that only the cells in interphase were counted. Values (means ± s.d.) are from three independent experiments. **P* < 0.05. Representative images from the α-adducin-depleted A431 cells (*A431/shAdd*) with abnormal nucleus are shown. Scale bars: 10 μm. (**C**) The A431 cells were fixed and stained for DNA and mitotic spindles (with anti-α-tubulin). The percentage of cells with disorganized mitotic spindles and abnormal chromosomal congregation/segregation in total counted mitotic cells (n > 200) was measured. Values (means ± s.d.) are from three independent experiments. **P* < 0.05. Representative images from the α-adducin-depleted A431 cells (*A431/shAdd*) with abnormal mitotic spindles and chromosomes are

shown. Scale bar: 10 μm. (**D**) The A431 cells were fixed and stained for DNA and centrosomes (with anti-γ-tubulin). The percentage of cells with abnormal centrosomes in total counted mitotic cells (n > 200) was measured. Values (means ± s.d.) are from three independent experiments. *P < 0.05. Representative images from the α-adducin-depleted A431 cells with abnormal centrosomes are shown. Scale bar: 5 μm. (**E**) Association of α-adducin with mitotic spindles. A431 cells were fixed and stained for α-adducin and α-tubulin. Representative images from mitotic cells in metaphase and telophase are shown.

Chen et al., Figure 1

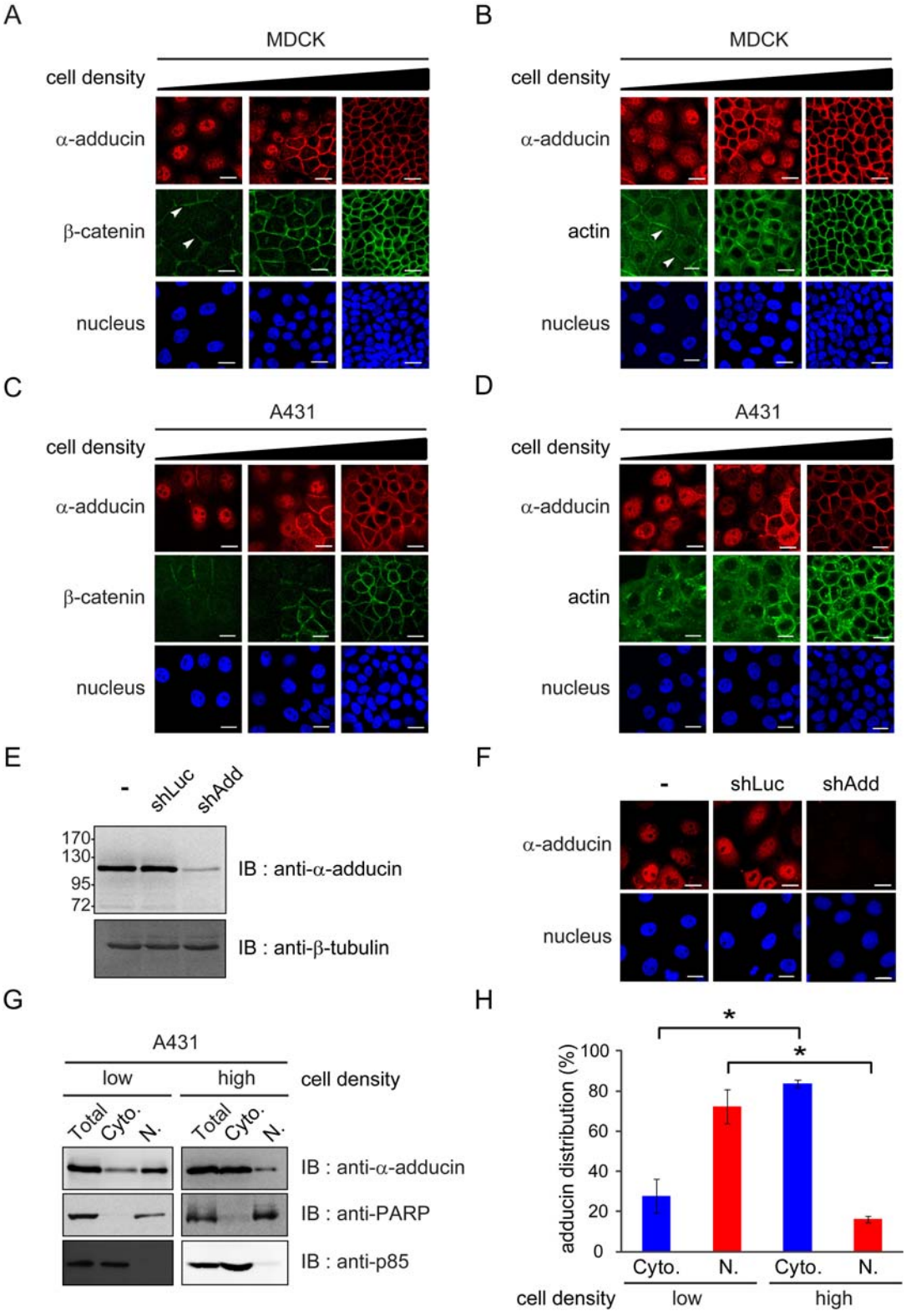

Chen et al., Figure 2

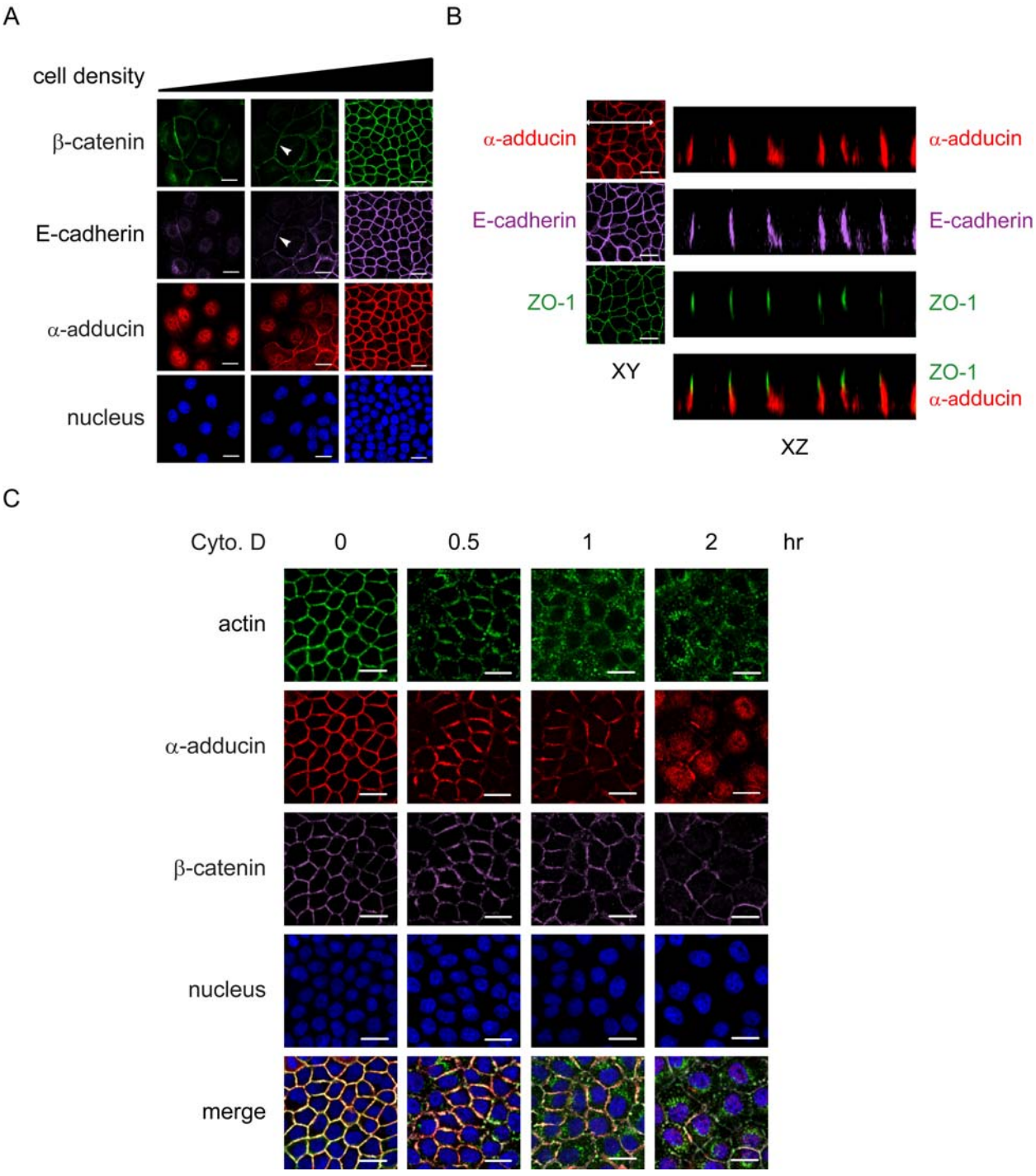

Chen et al., Figure 3

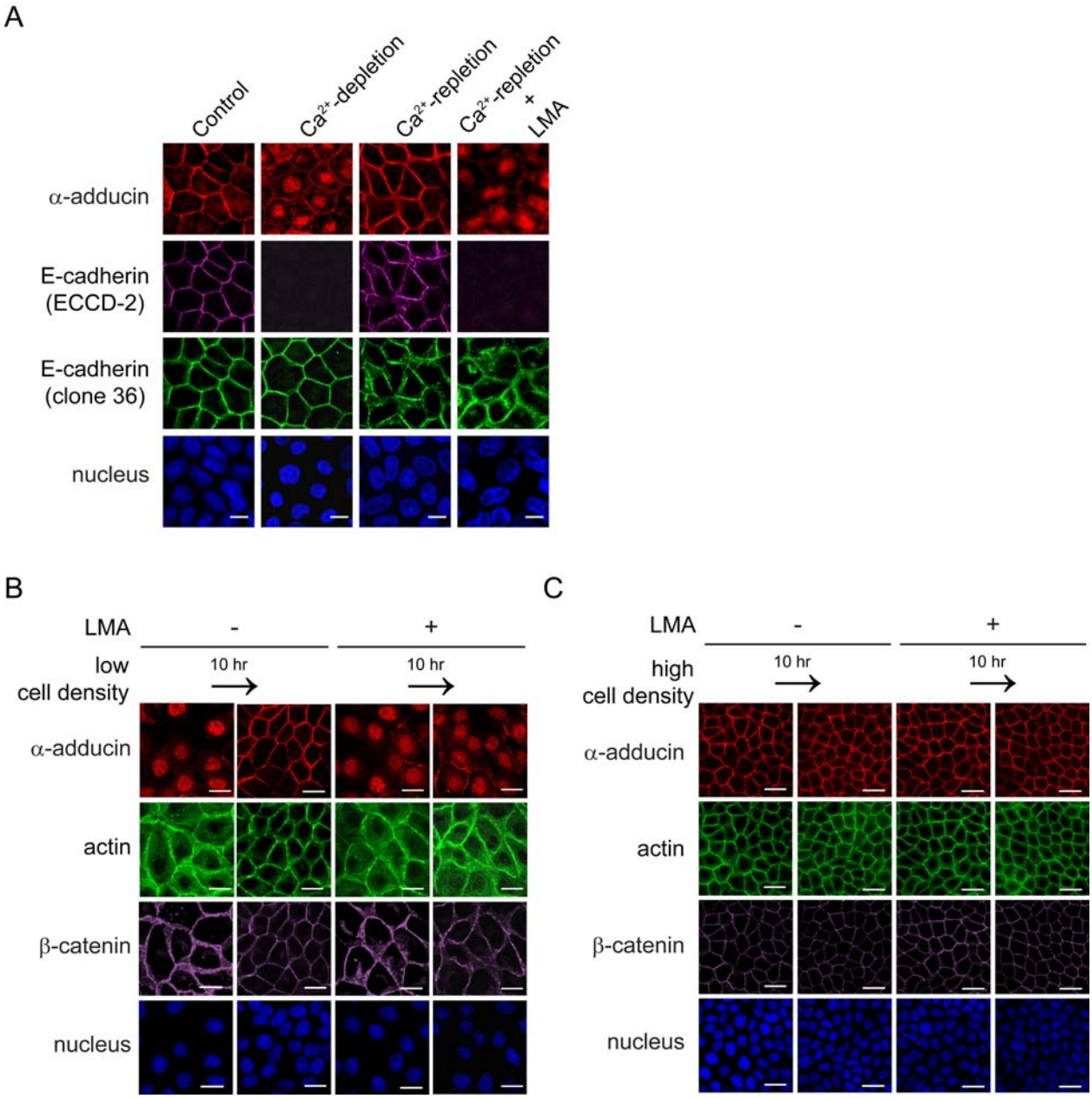

Chen et al., Figure 4

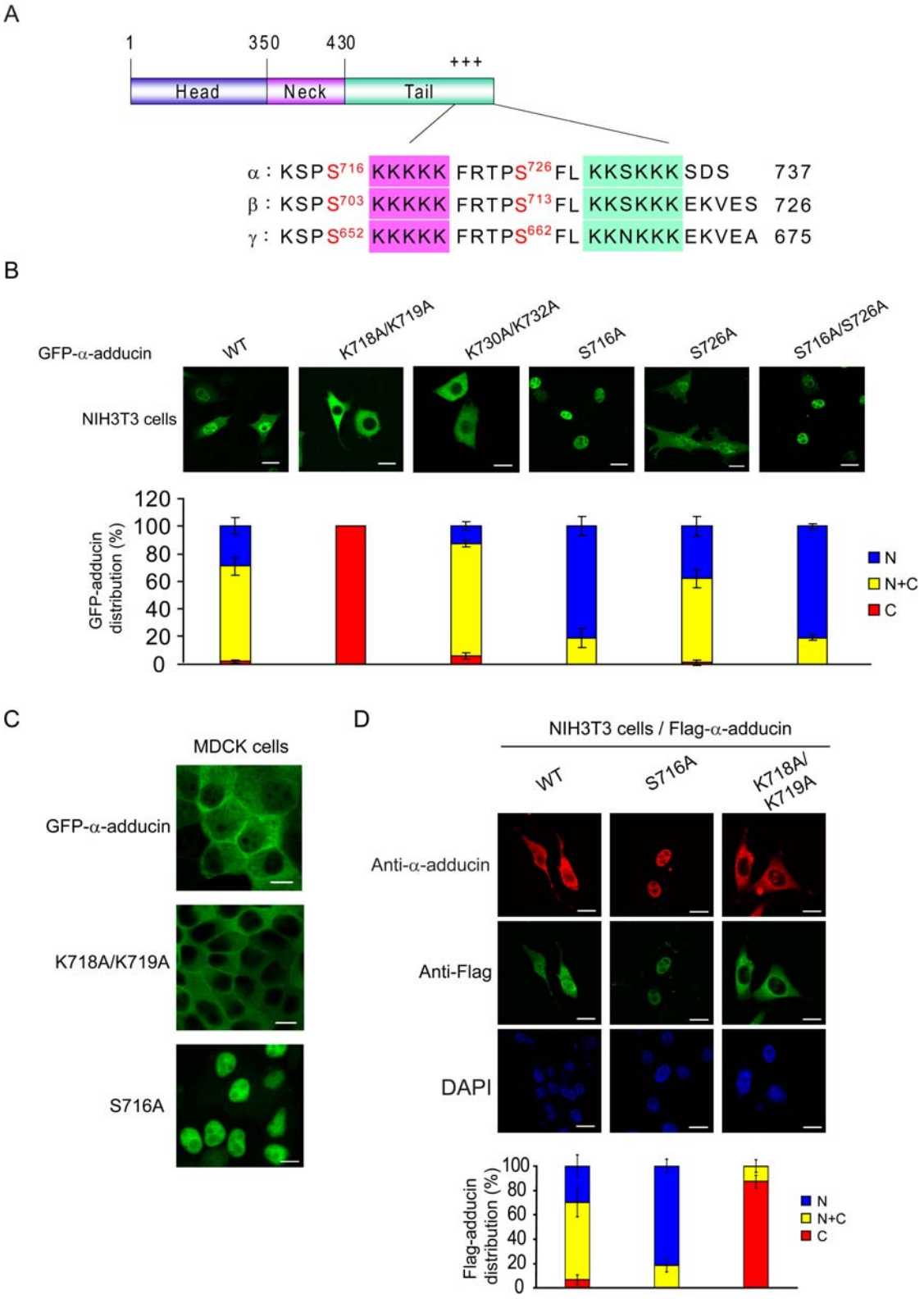

Chen et al., Figure 5

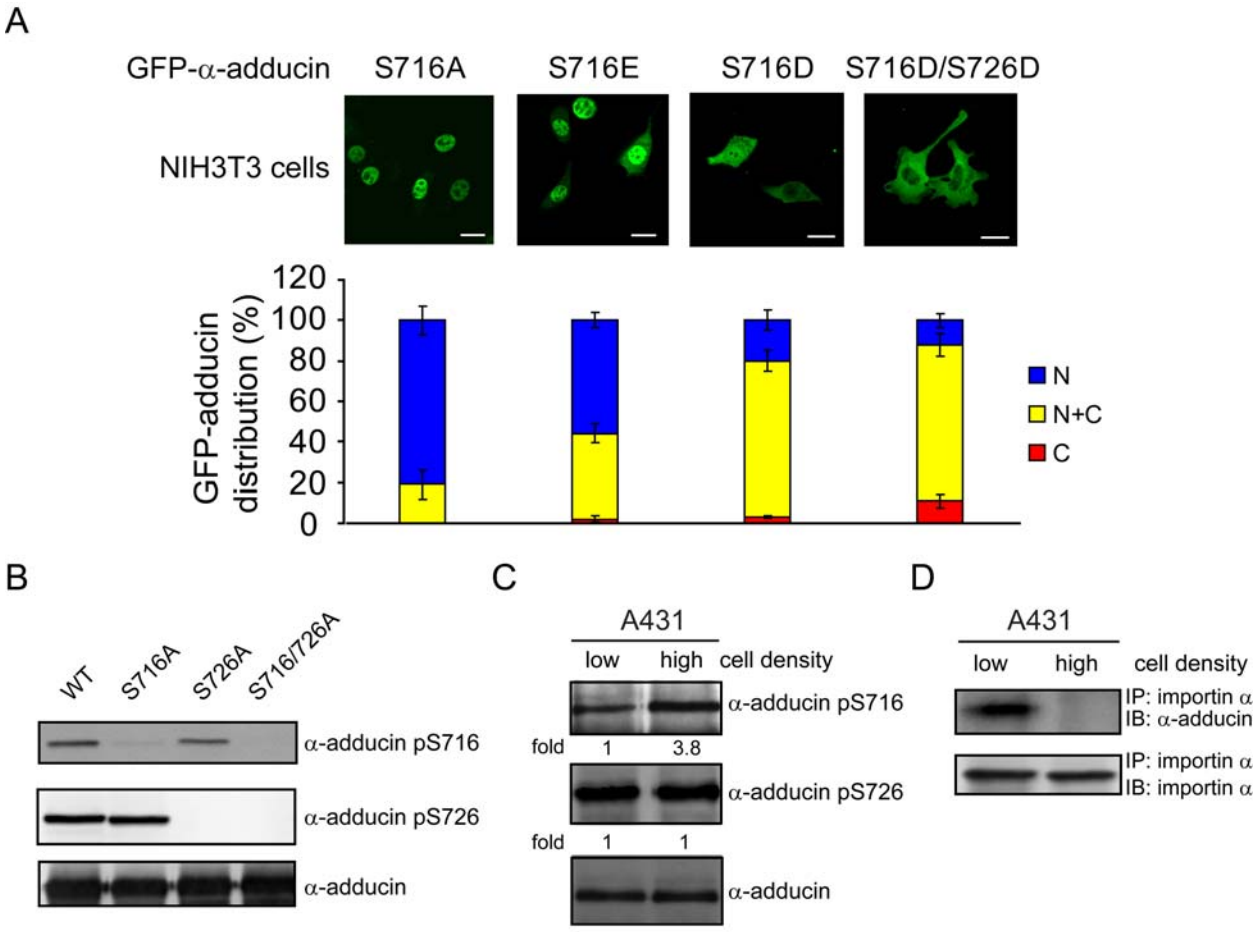

Chen et al., Figure 6

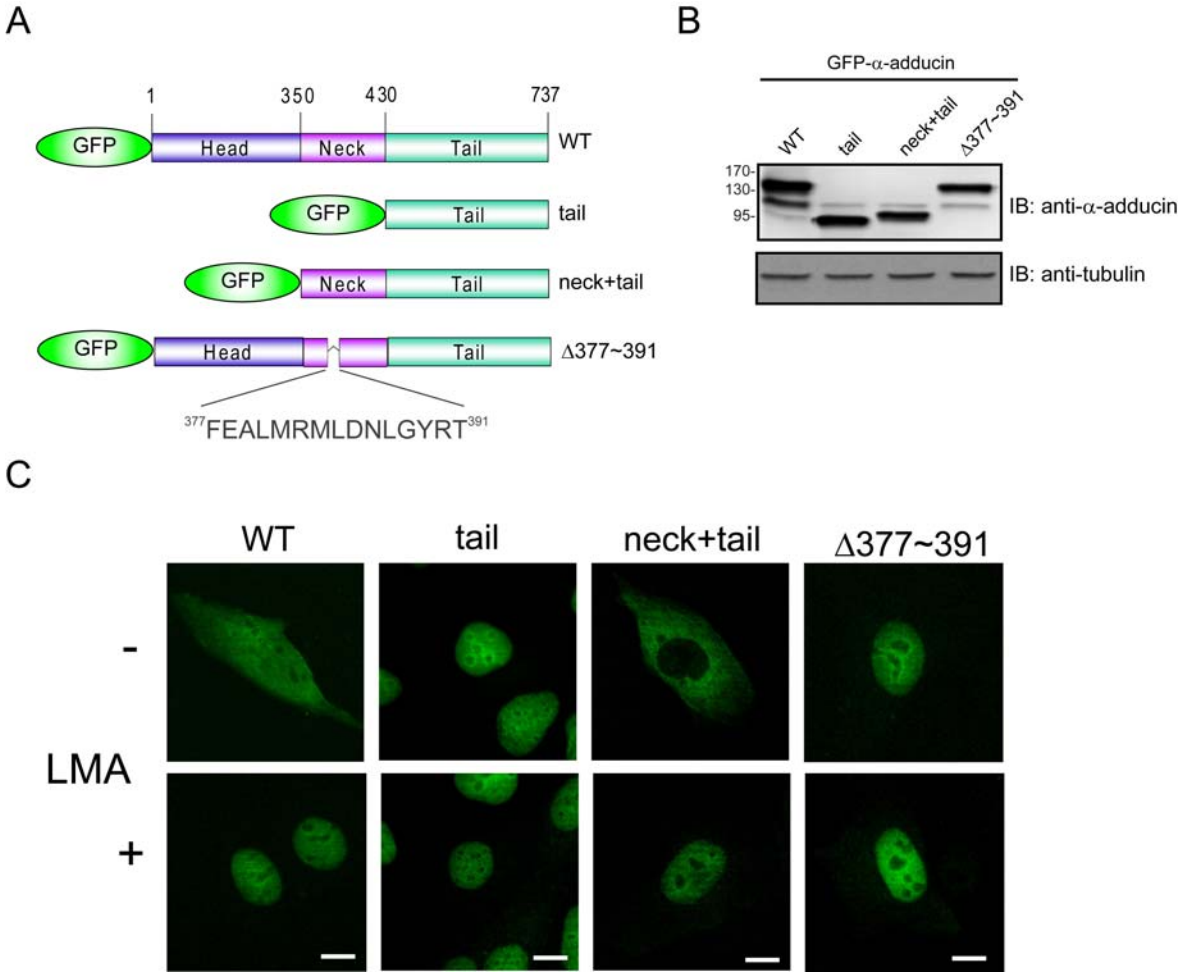

Chen et al., Figure 7

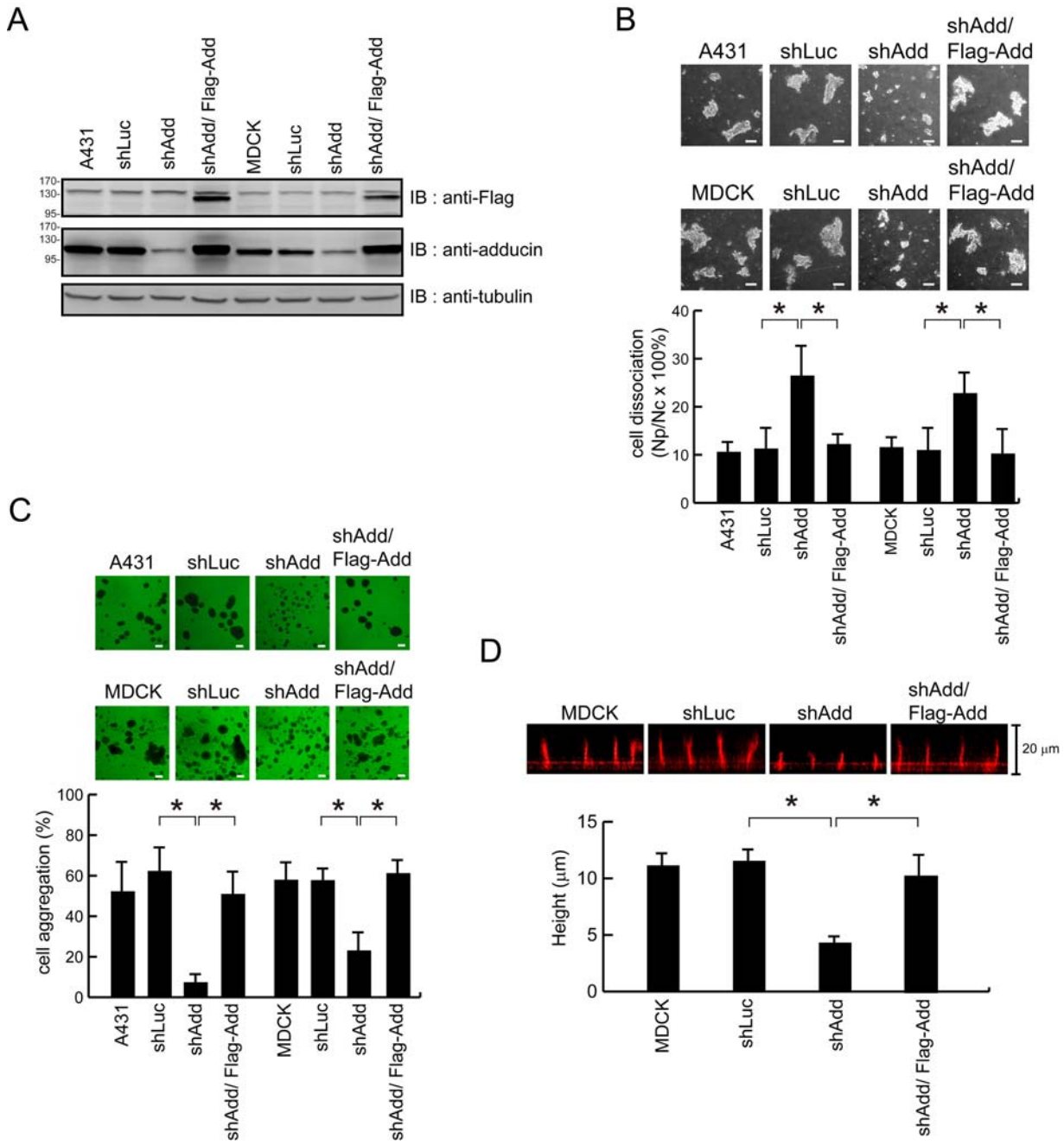

Chen et al., Figure 8